

EUROPEAN ORGANIZATION FOR NUCLEAR RESEARCH

CERN-EP-2001-093

7 December 2001

Search for Leptoquarks in Electron-Photon Scattering at $\sqrt{s_{ee}}$ up to 209 GeV at LEP

The OPAL Collaboration

Abstract

Searches for first generation scalar and vector leptoquarks, and for squarks in R-parity violating SUSY models with the direct decay of the squark into Standard Model particles, have been performed using e^+e^- collisions collected with the OPAL detector at LEP at e^+e^- centre-of-mass energies between 189 and 209 GeV. No excess of events is found over the expectation from Standard Model background processes. Limits are computed on the leptoquark couplings for different values of the branching ratio to electron-quark final states.

(To be submitted to Physics Letters)

arXiv:hep-ex/0112024v1 18 Dec 2001

The OPAL Collaboration

G. Abbiendi², C. Ainsley⁵, P.F. Åkesson³, G. Alexander²², J. Allison¹⁶,
G. Anagnostou¹, K.J. Anderson⁹, S. Arceci¹⁷, S. Asai²³, D. Axen²⁷,
G. Azuelos^{18,a}, I. Bailey²⁶, E. Barberio⁸, R.J. Barlow¹⁶, R.J. Batley⁵, P. Bechtel²⁵,
T. Behnke²⁵, K.W. Bell²⁰, P.J. Bell¹, G. Bella²², A. Bellerive⁶, G. Benelli⁴,
S. Bethke³², O. Biebel³², I.J. Bloodworth¹, O. Boeriu¹⁰, P. Bock¹¹, J. Böhme²⁵,
D. Bonacorsi², M. Boutemeur³¹, S. Braibant⁸, L. Brigliadori², R.M. Brown²⁰,
H.J. Burckhart⁸, J. Cammin³, S. Campana⁴, R.K. Carnegie⁶, B. Caron²⁸,
A.A. Carter¹³, J.R. Carter⁵, C.Y. Chang¹⁷, D.G. Charlton^{1,b}, P.E.L. Clarke¹⁵,
E. Clay¹⁵, I. Cohen²², J. Couchman¹⁵, A. Csilling^{8,i}, M. Cuffiani², S. Dado²¹,
G.M. Dallavalle², S. Dallison¹⁶, A. De Roeck⁸, E.A. De Wolf⁸, P. Dervan¹⁵,
K. Desch²⁵, B. Dienes³⁰, M. Donkers⁶, J. Dubbert³¹, E. Duchovni²⁴, G. Duckeck³¹,
I.P. Duerdoth¹⁶, E. Etzion²², F. Fabbri², L. Feld¹⁰, P. Ferrari¹², F. Fiedler⁸,
I. Fleck¹⁰, M. Ford⁵, A. Frey⁸, A. Fürties⁸, D.I. Futyan¹⁶, P. Gagnon¹²,
J.W. Gary⁴, G. Gaycken²⁵, C. Geich-Gimbel³, G. Giacomelli², P. Giacomelli²,
M. Giunta⁴, J. Goldberg²¹, K. Graham²⁶, E. Gross²⁴, J. Grunhaus²², M. Gruwé⁸,
P.O. Günther³, A. Gupta⁹, C. Hajdu²⁹, M. Hamann²⁵, G.G. Hanson¹²,
K. Harder²⁵, A. Harel²¹, M. Harin-Dirac⁴, M. Hauschild⁸, J. Hauschildt²⁵,
C.M. Hawkes¹, R. Hawkings⁸, R.J. Hemingway⁶, C. Hensel²⁵, G. Herten¹⁰,
R.D. Heuer²⁵, J.C. Hill⁵, K. Hoffman⁹, R.J. Homer¹, D. Horváth^{29,c},
K.R. Hossain²⁸, R. Howard²⁷, P. Hüntemeyer²⁵, P. Igo-Kemenes¹¹, K. Ishii²³,
A. Jawahery¹⁷, H. Jeremie¹⁸, C.R. Jones⁵, P. Jovanovic¹, T.R. Junk⁶,
N. Kanaya²⁶, J. Kanzaki²³, G. Karapetian¹⁸, D. Karlen⁶, V. Kartvelishvili¹⁶,
K. Kawagoe²³, T. Kawamoto²³, R.K. Keeler²⁶, R.G. Kellogg¹⁷, B.W. Kennedy²⁰,
D.H. Kim¹⁹, K. Klein¹¹, A. Klier²⁴, S. Kluth³², T. Kobayashi²³, M. Kobel³,
T.P. Kokott³, S. Komamiya²³, L. Kormos²⁶, R.V. Kowalewski²⁶, T. Krämer²⁵,
T. Kress⁴, P. Krieger^{6,0}, J. von Krogh¹¹, D. Krop¹², T. Kuhl²⁵, M. Kupper²⁴,
P. Kyberd¹³, G.D. Lafferty¹⁶, H. Landsman²¹, D. Lanske¹⁴, I. Lawson²⁶,
J.G. Layter⁴, A. Leins³¹, D. Lellouch²⁴, J. Letts¹², L. Levinson²⁴, J. Lillich¹⁰,
C. Littlewood⁵, S.L. Lloyd¹³, F.K. Loebinger¹⁶, J. Lu²⁷, J. Ludwig¹⁰,
A. Macchiolo¹⁸, A. Macpherson^{28,l}, W. Mader³, S. Marcellini², T.E. Marchant¹⁶,
A.J. Martin¹³, J.P. Martin¹⁸, G. Martinez¹⁷, G. Masetti², T. Mashimo²³,
P. Mättig²⁴, W.J. McDonald²⁸, J. McKenna²⁷, T.J. McMahon¹,
R.A. McPherson²⁶, F. Meijers⁸, P. Mendez-Lorenzo³¹, W. Menges²⁵,
F.S. Merritt⁹, H. Mes^{6,a}, A. Michelini², S. Mihara²³, G. Mikenberg²⁴,
D.J. Miller¹⁵, S. Moed²¹, W. Mohr¹⁰, T. Mori²³, A. Mutter¹⁰, K. Nagai¹³,
I. Nakamura²³, H.A. Neal³³, R. Nisius⁸, S.W. O’Neale¹, A. Oh⁸, A. Okpara¹¹,
M.J. Oreglia⁹, S. Orito²³, C. Pahl³², G. Pásztor^{8,i}, J.R. Pater¹⁶, G.N. Patrick²⁰,
J.E. Pilcher⁹, J. Pinfold²⁸, D.E. Plane⁸, B. Poli², J. Polok⁸, O. Pooth⁸, A. Quadt³,
K. Rabbertz⁸, C. Rembser⁸, P. Renkel²⁴, H. Rick⁴, N. Rodning²⁸, J.M. Roney²⁶,
S. Rosati³, K. Roscoe¹⁶, Y. Rozen²¹, K. Runge¹⁰, D.R. Rust¹², K. Sachs⁶,

T. Saeki²³, O. Sahr³¹, E.K.G. Sarkisyan^{8,m}, A.D. Schaile³¹, O. Schaile³¹,
P. Scharff-Hansen⁸, M. Schröder⁸, M. Schumacher²⁵, C. Schwick⁸, W.G. Scott²⁰,
R. Seuster^{14,g}, T.G. Shears^{8,j}, B.C. Shen⁴, C.H. Shepherd-Themistocleous⁵,
P. Sherwood¹⁵, A. Skuja¹⁷, A.M. Smith⁸, G.A. Snow¹⁷, R. Sobie²⁶,
S. Söldner-Rembold^{10,e}, S. Spagnolo²⁰, F. Spano⁹, M. Sproston²⁰, A. Stahl³,
K. Stephens¹⁶, D. Strom¹⁹, R. Ströhmer³¹, B. Surrow²⁵, S. Tarem²¹, M. Tasevsky⁸,
R.J. Taylor¹⁵, R. Teuscher⁹, J. Thomas¹⁵, M.A. Thomson⁵, E. Torrence¹⁹,
D. Toya²³, T. Trefzger³¹, A. Tricoli², I. Trigger⁸, Z. Trócsányi^{30,f}, E. Tsur²²,
M.F. Turner-Watson¹, I. Ueda²³, B. Ujvári^{30,f}, B. Vachon²⁶, C.F. Vollmer³¹,
P. Vanmerem¹⁰, M. Verzocchi¹⁷, H. Voss⁸, J. Vossebeld⁸, D. Waller⁶, C.P. Ward⁵,
D.R. Ward⁵, P.M. Watkins¹, A.T. Watson¹, N.K. Watson¹, P.S. Wells⁸,
T. Wengler⁸, N. Wermes³, D. Wetterling¹¹, G.W. Wilson^{16,n}, J.A. Wilson¹,
T.R. Wyatt¹⁶, S. Yamashita²³, V. Zacek¹⁸, D. Zer-Zion^{8,k}

¹School of Physics and Astronomy, University of Birmingham, Birmingham B15 2TT, UK

²Dipartimento di Fisica dell' Università di Bologna and INFN, I-40126 Bologna, Italy

³Physikalisches Institut, Universität Bonn, D-53115 Bonn, Germany

⁴Department of Physics, University of California, Riverside CA 92521, USA

⁵Cavendish Laboratory, Cambridge CB3 0HE, UK

⁶Ottawa-Carleton Institute for Physics, Department of Physics, Carleton University, Ottawa, Ontario K1S 5B6, Canada

⁸CERN, European Organisation for Nuclear Research, CH-1211 Geneva 23, Switzerland

⁹Enrico Fermi Institute and Department of Physics, University of Chicago, Chicago IL 60637, USA

¹⁰Fakultät für Physik, Albert Ludwigs Universität, D-79104 Freiburg, Germany

¹¹Physikalisches Institut, Universität Heidelberg, D-69120 Heidelberg, Germany

¹²Indiana University, Department of Physics, Swain Hall West 117, Bloomington IN 47405, USA

¹³Queen Mary and Westfield College, University of London, London E1 4NS, UK

¹⁴Technische Hochschule Aachen, III Physikalisches Institut, Sommerfeldstrasse 26-28, D-52056 Aachen, Germany

¹⁵University College London, London WC1E 6BT, UK

¹⁶Department of Physics, Schuster Laboratory, The University, Manchester M13 9PL, UK

¹⁷Department of Physics, University of Maryland, College Park, MD 20742, USA

¹⁸Laboratoire de Physique Nucléaire, Université de Montréal, Montréal, Quebec H3C 3J7, Canada

¹⁹University of Oregon, Department of Physics, Eugene OR 97403, USA

²⁰CLRC Rutherford Appleton Laboratory, Chilton, Didcot, Oxfordshire OX11 0QX, UK

²¹Department of Physics, Technion-Israel Institute of Technology, Haifa 32000, Israel

²²Department of Physics and Astronomy, Tel Aviv University, Tel Aviv 69978, Israel

²³International Centre for Elementary Particle Physics and Department of Physics, University of Tokyo, Tokyo 113-0033, and Kobe University, Kobe 657-8501, Japan

²⁴Particle Physics Department, Weizmann Institute of Science, Rehovot 76100, Israel

²⁵Universität Hamburg/DESY, II Institut für Experimental Physik, Notkestrasse 85, D-22607 Hamburg, Germany

²⁶University of Victoria, Department of Physics, P O Box 3055, Victoria BC V8W 3P6, Canada

²⁷University of British Columbia, Department of Physics, Vancouver BC V6T 1Z1, Canada

²⁸University of Alberta, Department of Physics, Edmonton AB T6G 2J1, Canada

²⁹Research Institute for Particle and Nuclear Physics, H-1525 Budapest, P O Box 49, Hungary

³⁰Institute of Nuclear Research, H-4001 Debrecen, P O Box 51, Hungary

³¹Ludwigs-Maximilians-Universität München, Sektion Physik, Am Coulombwall 1, D-85748 Garching, Germany

³²Max-Planck-Institute für Physik, Föhring Ring 6, 80805 München, Germany

³³Yale University, Department of Physics, New Haven, CT 06520, USA

^a and at TRIUMF, Vancouver, Canada V6T 2A3

^b and Royal Society University Research Fellow

^c and Institute of Nuclear Research, Debrecen, Hungary

^e and Heisenberg Fellow

^f and Department of Experimental Physics, Lajos Kossuth University, Debrecen, Hungary

^g and MPI München

ⁱ and Research Institute for Particle and Nuclear Physics, Budapest, Hungary

^j now at University of Liverpool, Dept of Physics, Liverpool L69 3BX, UK

^k and University of California, Riverside, High Energy Physics Group, CA 92521, USA

^l and CERN, EP Div, 1211 Geneva 23

^m and Universitaire Instelling Antwerpen, Physics Department, B-2610 Antwerpen, Belgium

ⁿ now at University of Kansas, Dept of Physics and Astronomy, Lawrence, KS 66045, USA

^o now at University of Toronto, Dept of Physics, Toronto, Canada

1 Introduction

The observed symmetry between the lepton and quark sectors in the Standard Model is not yet understood, but could be interpreted as a hint for common underlying structures. Consequently, many extensions of the Standard Model postulate the existence of leptoquarks (LQ), which are coloured spin 0 or spin 1 particles carrying both baryon (B) and lepton (L) quantum numbers. The Buchmüller-Rückl-Wyler (BRW) model [1] adopted in this paper assumes lepton and baryon number conservation. Two additional assumptions on the leptoquark couplings are made in the following: only the couplings λ within one generation of fermions are assumed to be non-zero (to respect lepton flavour conservation), and only the case of chiral couplings is considered, i.e. it is assumed that the product $\lambda_R \lambda_L$ of couplings to left-handed and right-handed leptons vanishes (to respect lepton universality). With the latter assumption the branching ratio β_e of leptoquarks to final states with a charged lepton is restricted, as shown in Table 1.

This paper presents the results of a search for single production of leptoquarks in e^+e^- collisions with the OPAL detector at LEP. Leptoquarks would be produced by an electron-quark¹ fusion. In the dominant diagram, which is shown schematically in Figure 1, the quark is the result of a process where one of the incoming leptons radiates a photon which subsequently fluctuates into a hadronic state [3]. Under the above assumptions on the leptoquark couplings, only first generation leptoquarks coupled to electrons could be produced in electron-photon scattering, and they would decay into either an electron and a quark or into a neutrino and a quark. Therefore the main signature of single leptoquark events is one hadronic jet balanced in the transverse plane either by one isolated electron or by missing transverse energy due to the neutrino. The hadronic photon remnant would disappear down the beam-pipe or add some activity in the forward region of the detector.

In supersymmetric models with R-parity violation, scalar quarks (squarks) have the same production mechanism as some leptoquarks. The topology of events with single squark production depends on the squark decays; if R-parity conserving decays can be neglected, the results on the left-handed couplings for leptoquarks presented in this paper apply also to the corresponding squark states. In the following, leptoquarks and the corresponding squark states with R-parity violating decays are generically referred to as leptoquarks.

Experiments at LEP [4, 5], HERA [6], and the Tevatron [7] have searched for leptoquarks. We present a search for leptoquarks with $M_{LQ} > 80 \text{ GeV}$ in

¹Charge conjugation is implied throughout this paper for all particles, e.g. positrons are also referred to as electrons.

scalar LQ (\tilde{q})	charge	F	coupling and decay mode	β_e
S_0 (or \tilde{d}_R)	$-1/3$	2	$\lambda_L : e_L^- u, \nu_L d$ $\lambda_R : e_R^- u$	$1/2$ 1
\tilde{S}_0	$-4/3$	2	$\lambda_R : e_R^- d$	1
$\tilde{S}_{1/2}$ (or \tilde{d}_L)	$+1/3$	0	$\lambda_L : \nu_L \bar{d}$	0
$\tilde{S}_{1/2}$ (or \tilde{u}_L)	$-2/3$	0	$\lambda_L : e_L^- \bar{d}$	1
S_1	$+2/3$	2	$\lambda_L : \nu_L u$	0
	$-1/3$		$\lambda_L : \nu_L d, e_L^- u$	$1/2$
	$-4/3$		$\lambda_L : e_L^- d$	1
$S_{1/2}$	$-2/3$	0	$\lambda_L : \nu_L \bar{u}$	0
	$-5/3$		$\lambda_R : e_R^- \bar{d}$	1
			$\lambda_L : e_L^- \bar{u}$	1
			$\lambda_R : e_R^- \bar{u}$	1

vector LQ	charge	F	coupling and decay mode	β_e
$V_{1/2}$	$-1/3$	2	$\lambda_L : \nu_L d$	0
	$-4/3$		$\lambda_R : e_R^- u$	1
			$\lambda_L : e_L^- d$	1
			$\lambda_R : e_R^- d$	1
$\tilde{V}_{1/2}$	$+2/3$	2	$\lambda_L : \nu_L u$	0
	$-1/3$		$\lambda_L : e_L^- u$	1
V_0	$-2/3$	0	$\lambda_L : e_L^- \bar{d}, \nu_L \bar{u}$	$1/2$
			$\lambda_R : e_R^- \bar{d}$	1
V_1	$+1/3$	0	$\lambda_L : \nu_L \bar{d}$	0
	$-2/3$		$\lambda_L : e_L^- \bar{d}, \nu_L \bar{u}$	$1/2$
	$-5/3$		$\lambda_L : e_L^- \bar{u}$	1
\tilde{V}_0	$-5/3$	0	$\lambda_R : e_R^- \bar{u}$	1

Table 1: The first generation scalar (S) leptoquarks/squarks and vector (V) leptoquarks in the BRW model according to the nomenclature in [2] with their electric charge in units of e and fermion number $F = L + 3B$. For each possible non-zero coupling λ the decay modes and the corresponding branching ratio β_e for the decay into an electron and a quark are also listed. The restrictions on the values of β_e arise from the assumption of chiral couplings.

electron-photon scattering using data corresponding to an integrated luminosity of 612.3 pb^{-1} at e^+e^- centre-of-mass energies between 189 and 209 GeV. The data sample is split into eight bins with average e^+e^- centre-of-mass energies of 188.6 GeV, 191.6 GeV, 195.5 GeV, 199.5 GeV, 201.6 GeV, 204.9 GeV, 206.5 GeV, and 208.0 GeV. This paper extends the previous OPAL analysis [4] to the highest LEP centre-of-mass energies and uses refined experimental techniques. The data used in [4] are included in this analysis and thus the results from [4] are superseded.

2 The OPAL Detector

The OPAL detector is described in detail elsewhere [8]. It is a multipurpose apparatus with almost complete solid angle coverage. The central detector consists of two layers of silicon micro-strip detectors [9] and a system of gas-filled tracking chambers in a 0.435 T solenoidal magnetic field which is parallel to the beam axis.

A lead-glass electromagnetic calorimeter with a presampler is located outside the magnet coil. In combination with the forward calorimeters, the forward scintillating tile counter [10], and the silicon-tungsten luminometer [11], a geometrical acceptance is provided down to 25 mrad from the beam direction. The silicon-tungsten luminometer measures the integrated luminosity using small-angle Bhabha scattering events [12]. The magnet return yoke is instrumented for hadron calorimetry, and is surrounded by several layers of muon chambers.

3 Monte Carlo Simulation

The Monte Carlo simulation of the process $e^+e^- \rightarrow \text{LQ} + \text{X} + e$ and the calculation of the production cross-section, defined as the sum of the cross-sections for the particle and antiparticle states, are performed with the program `ERATO-LQ` [13]. The hadronisation of the leptoquark decay products and the hadronic photon remnant is performed using `JETSET` [14]. Details of the Monte Carlo simulation of single leptoquark production and the calculation of the total cross-section can be found in [4]. Samples of 3000 signal events are generated for both scalar and vector leptoquark states, for both eq and νq final states, for e^+e^- centre-of-mass energies $\sqrt{s_{ee}}$ of 200 and 208 GeV, and for scaled leptoquark masses $x_{\text{LQ}} = m_{\text{LQ}}/\sqrt{s_{ee}}$ of $x_{\text{LQ}} = 0.42, 0.53, 0.63, 0.74, 0.85, 0.90, 0.95,$ and 0.98 , making a total of 64 samples. For a given scaled leptoquark mass the event properties depend only weakly on the centre-of-mass energy.

To study Standard Model background processes, two-fermion hadronic events ($e^+e^- \rightarrow q\bar{q}(\gamma)$) are simulated with `PYTHIA 5.722` [14], while the $e^+e^- \rightarrow \tau^+\tau^-$ and $e^+e^- \rightarrow e^+e^-$ processes are generated with `KORALZ 4.02` [15] and `BHWIDE` [16], respectively. Deep inelastic hadronic two-photon background events in the range $Q^2 > 4.5 \text{ GeV}^2$, including charged current deep inelastic scattering (CC DIS) events, are simulated with `HERWIG 5.8` [17], while `PHOJET 1.10` [18] is used to generate hadronic two-photon events in the range $Q^2 < 4.5 \text{ GeV}^2$. For leptonic two-photon events, `Vermaseren` [19] is used. Final states with four-fermion production are simulated with `grc4f` [20].

All Monte Carlo events are passed through a full detector simulation [21] and the same reconstruction algorithms as the real data.

4 Event Analysis

We search for events with one hadronic jet and either an electron or missing energy balancing the transverse momentum of this jet. The analysis uses tracks reconstructed in the central tracking devices and clusters measured in the calorimeters and forward detectors. The selection of tracks and clusters is similar to that used in previous OPAL analyses. In addition to quality requirements [4], tracks must have more than 20 hits in the central jet chamber, more than half the number of hits expected given the polar angle of the track and the geometry of the jet chamber, and a transverse momentum with respect to the beam direction of more than 120 MeV. Calorimeter clusters must pass energy threshold cuts to suppress noise. To avoid double counting of particle energies, a matching algorithm between tracks and clusters is applied [22].

Jets are reconstructed from the tracks and clusters using the Durham [23] and cone [24] algorithms. The y parameter value y_{12} (y_{23}) where the transition from a one- to two-jet (two- to three-jet) event occurs is determined with the Durham algorithm. These parameters provide information on the event shape in the following analysis. A cone jet finder [24], requiring a minimum energy of 15 GeV in a cone of half-angle 1.0 radian is used to provide information on jet directions and energies. No requirement on the number of jets is made.

4.1 The Electron Plus Hadronic Jet Channel

Tracks are identified as electrons if more than 20 measurement samples can be used to determine the specific ionisation energy loss, dE/dx , if the dE/dx probability [25] for the electron hypothesis exceeds 1%, and if the ratio of the electron

energy measured in the electromagnetic calorimeter to the track momentum is between 0.7 and 2.0. In each event, the electron with the largest momentum is assumed to be the one from leptoquark decay.

Candidate leptoquark events are then selected based on the following cuts:

- EQ1) The event must contain more than five tracks, and the energy measured in the hadron calorimeter must exceed 1 GeV.
- EQ2) The ratio $\cancel{E}_T/E_{\text{vis}}$ of the missing transverse energy \cancel{E}_T and the visible energy E_{vis} has to be smaller than 0.2. This cut mainly reduces background from 4-fermion and two-photon events.
- EQ3) The event must contain an identified electron, and its energy E_e has to be larger than $0.2\sqrt{s_{ee}}$, where $\sqrt{s_{ee}}$ denotes the e^+e^- centre-of-mass energy. The energy of the cone jet containing the most energetic electron must not exceed the electron energy by more than 12% of the centre-of-mass energy. This ensures that isolated, energetic electrons are selected.
- EQ4) At least one cone jet not containing the electron is required, and the leptoquark is reconstructed from the electron and the most energetic other cone jet (quark jet). The quantity $\cos\theta_e^*$ is the cosine of the helicity angle between the electron in the leptoquark rest frame and the leptoquark flight direction in the laboratory frame. Since high-mass leptoquarks will be almost at rest in the laboratory, the finite energy and momentum resolution of the detector will produce an apparent leptoquark direction close to the jet or the electron direction. Therefore the distribution of $\cos\theta_e^*$ will be strongly peaked at ± 1 . To remove small-angle Bhabba events in which one electron produces a shower in the tracking chambers, the multiplicity of the quark jet (defined as the number of tracks plus unassociated clusters) is required to be larger than 10 for $|\cos\theta_e^*| > 0.95$ and $|\cos\theta_e| > 0.8$, where θ_e denotes the electron polar angle with respect to the outgoing electron beam².

The above cuts are applied for all centre-of-mass energies and leptoquark masses and states. To reject background further, an x_{LQ} -dependent likelihood is constructed, where the leptoquark mass is reconstructed as the invariant mass of the electron and the quark jet. The likelihood uses as inputs:

- the charge-signed cosine of the electron polar angle, $-q_e \cos\theta_e$,

²The OPAL coordinate system is defined as a right-handed Cartesian coordinate system, with the x axis pointing in the plane of the LEP collider towards the centre of the ring, and the z axis in the direction of the outgoing beam electrons.

- the quantity $\cos\theta_e^*$ defined above,
- the logarithm of y_{23} from the Durham jet finder,
- the cosine of the polar angle of a third jet in the event, if one exists³, multiplied by the sign of $\cos\theta_e$, and
- the ratio $\cancel{E}_T/E_{\text{vis}}$.

Monte Carlo samples that are statistically independent of those used in the efficiency determination are used to obtain the probability density to construct the likelihood function. Two-fermion events, four-fermion events, and two-photon events are considered as separate background hypotheses. The signal reference distributions for the likelihood for a given event should ideally be derived from Monte Carlo simulation of a leptoquark with a mass corresponding to the measured electron-jet mass of that event. Since the scaled electron-jet mass x_{LQ} of the event does not in general correspond to one of the signal Monte Carlo masses, bin-by-bin interpolation from the two Monte Carlo samples with x_{LQ} bracketing that of the measured event is used to determine the signal reference histograms used for its likelihood. For each event, the signal likelihood is calculated from the average of the scalar and vector leptoquark distributions at the reconstructed leptoquark mass. Finally, events are accepted if they pass a cut on the likelihood value $\mathcal{L} > 0.8$.

In Table 2, the number of data events and the expected number of Standard Model background events are shown after each selection cut. The selection efficiencies for two different scalar and vector leptoquark masses at 200 GeV e^+e^- centre-of-mass energy are also given. The likelihood interpolation technique described above was checked at each leptoquark mass simulated in the Monte Carlo by comparing the efficiency obtained when using reference histograms derived directly from the Monte Carlo at that mass to that obtained when the histograms were derived by interpolating the next two nearest simulated mass points. It was found that the interpolation method degrades the efficiency by about 15% for low-mass leptoquarks, while it has a very small effect for high-mass leptoquark. The efficiency for leptoquark detection is therefore reduced to account for this effect.

Figures 2a-e show the distributions of some of the cut variables for data, Standard Model background and the leptoquark state $S_{1/2}$ with two different scaled masses x_{LQ} . In general, good agreement between the data and Standard Model background is observed. The distribution of reconstructed leptoquark masses is shown in Figure 2f for events that pass all cuts. No significant excess is observed in the data.

³Events in which no third cone jet is found are collected in a separate bin.

events	selection steps (cumulative cuts)				
	(EQ1)	(EQ2)	(EQ3)	(EQ4)	$\mathcal{L} > 0.8$
signal efficiencies:					
scalar LQ, $m_{\text{LQ}} = 106.0$ GeV	72.6%	55.0%	39.8%	39.7%	$(15.6 \pm 1.1)\%$
scalar LQ, $m_{\text{LQ}} = 190.5$ GeV	79.4%	69.3%	57.3%	56.7%	$(49.2 \pm 2.7)\%$
vector LQ, $m_{\text{LQ}} = 106.0$ GeV	66.5%	46.8%	32.4%	32.4%	$(9.8 \pm 0.8)\%$
vector LQ, $m_{\text{LQ}} = 190.5$ GeV	70.6%	61.9%	51.5%	51.1%	$(47.7 \pm 2.7)\%$
expected background events:					
$e^+e^- \rightarrow 2$ fermions	46391	17682	94.0	91.5	9.1 ± 2.9
$e^+e^- \rightarrow 4$ fermions	12800	5111	431	428	23.7 ± 7.4
two-photon	765676	5702	71.0	67.3	11.9 ± 3.9
charged-current DIS	25.8	0.1	< 0.1	< 0.1	< 0.1
total expected background	824892	28496	596	587	44.7 ± 14.0
observed events:					
data	735325	28888	562	536	43

Table 2: Selection efficiencies in the eq channel. The listed efficiencies are for $\sqrt{s_{ee}} = 200$ GeV. The remaining number of data events and the expected number of background events are also listed after each selection cut. All event numbers are quoted after a loose event preselection in which more than 2 tracks, more than 0.1 GeV total energy in the hadron calorimeter, and an identified electron are required. The errors are the total systematic uncertainties including the Monte Carlo statistical error. The component which is not due to Monte Carlo statistics is correlated between the separate contributions to the background. The determination of the systematic errors is discussed in Section 5.

4.2 The Neutrino Plus Hadronic Jet Channel

In this case we search for events with a single hadronic jet whose transverse energy is balanced by missing transverse energy. The kinematic properties of leptoquark events decaying to νq final states do not depend strongly on the leptoquark mass, so the selection is independent of the reconstructed transverse mass and no likelihood is used. The selection cuts are:

- NQ1) As in the eq channel, the event must contain more than five tracks, and the energy measured in the hadron calorimeter must exceed 1 GeV.
- NQ2) The presence of at least one cone jet is required. To ensure that the event is well contained in the detector, the polar angle of the missing momentum vector must satisfy $|\cos\theta(\vec{p})| < 0.95$, and the polar angle of the most energetic cone jet $|\cos\theta_{\text{jet } 1}| < 0.85$.
- NQ3) The transverse mass m_T^{LQ} of the leptoquark is calculated from the transverse momentum $p_T^{\text{jet } 1}$ of the most energetic cone jet in the event and the missing transverse momentum \cancel{p}_T of the event, $m_T^{\text{LQ}} = \sqrt{2p_T^{\text{jet } 1}\cancel{p}_T(1 - \cos\alpha)}$, where α is the opening angle between $p_T^{\text{jet } 1}$ and \cancel{p}_T . For one-jet events, there is a strong correlation between m_T^{LQ} and \cancel{E}_T , and the ratio is required to satisfy $0.497 < \cancel{E}_T/m_T^{\text{LQ}} < 0.512$. The cut is chosen to be asymmetric to retain good efficiency for low-mass leptoquarks.
- NQ4) Finally, the requirement of $\ln y_{23} + 1.4 \cdot \ln y_{12} < -10.5$ is used to select events with a one-jet topology, as shown in Figure 3c. The factor of 1.4 has been found to give good separation of signal and background.

Table 3 shows the numbers of data and expected background events normalised to the data luminosity after each cut. The efficiencies for two different scalar and vector leptoquark masses are also given.

Figures 3a-c show some of the selection variables for the data, the Standard Model background and the leptoquark state $S_{1/2}$ with two different scaled masses x_{LQ} . The expected background describes the data well. The transverse mass distribution of the selected leptoquark candidates is shown in Figure 3d after all cuts. No significant excess is observed in the data. Therefore, limits are calculated on the production of leptoquarks as discussed in the following sections.

events	selection steps (cumulative cuts)			
	(NQ1)	(NQ2)	(NQ3)	(NQ4)
signal efficiencies:				
scalar LQ, $m_{\text{LQ}} = 106.0$ GeV	56.1%	49.7%	41.8%	$(35.5 \pm 4.3)\%$
scalar LQ, $m_{\text{LQ}} = 190.5$ GeV	66.6%	61.7%	56.6%	$(56.5 \pm 6.3)\%$
vector LQ, $m_{\text{LQ}} = 106.0$ GeV	55.1%	48.8%	42.5%	$(32.1 \pm 3.9)\%$
vector LQ, $m_{\text{LQ}} = 190.5$ GeV	59.0%	55.9%	51.3%	$(51.3 \pm 5.8)\%$
expected background events:				
$e^+e^- \rightarrow 2$ fermions	17936	6887	19.1	0.2 ± 0.1
$e^+e^- \rightarrow 4$ fermions	5721	3886	226	20.5 ± 6.6
two-photon	14517	209	5.8	< 0.4
charged-current DIS	16.9	12.1	8.8	6.0 ± 1.9
total expected background	38192	10994	259	26.7 ± 8.6
observed events:				
data	43094	11303	292	25

Table 3: Selection efficiencies in the νq channel. The listed efficiencies are for $\sqrt{s_{ee}} = 200$ GeV. Also shown are the remaining number of data events and the expected number of background events after each selection cut. All event numbers are quoted after a loose event preselection in which more than 2 tracks, more than 0.1 GeV total energy in the hadron calorimeter, $|\cos\theta(\vec{p})| < 0.99$, and $0.48 < \cancel{E}_T/m_T^{\text{LQ}} < 0.52$ is required. The errors are the total systematic uncertainties including the Monte Carlo statistical error. The component which is not due to Monte Carlo statistics is correlated between the separate contributions to the background. The determination of the systematic errors is discussed in Section 5.

5 Systematic Uncertainties

Systematic uncertainties arise from (1) the luminosity measurement, (2) the limited size of the simulated event samples, (3) the modelling of the signal processes, and (4) the modelling of the Standard Model backgrounds.

The integrated luminosity has been varied by its uncertainty of 0.2%. The resulting error is negligible. The statistical error of around 1% on the signal efficiencies is taken into account.

In the simulation of signal events described in Section 3, the leptoquark is assumed to decay before hadronisation. However, if the leptoquark mass and couplings to fermions are small, the hadronisation process could begin before the leptoquark decay. This leads to differences in the event properties, notably in the number of charged particle tracks per event. Similar to [4], the dependence of the efficiency on the fragmentation modelling has been studied with a special version of PYTHIA where the two cases have been implemented [26]. The resulting uncertainty in the efficiency is 5% for eq states and 11% for ν q states. Also, the parameters of the cone jet finder have been varied (the minimum jet energy by (15 ± 5) GeV and the cone half angle by (1.0 ± 0.35)) in the signal Monte Carlo. This results in an uncertainty of 1% for eq final states and 1% - 4% for ν q states.

To assess the uncertainties in the modelling of the background, the simulated distribution of each quantity which is used in the selection (except for the variable $\ln y_{23} + 1.4 \cdot \ln y_{12}$ in the ν q channel) is reweighted in turn to match the data distribution after all preceding cuts in the selection. The selection (cuts and likelihood) is left unchanged. The difference between the efficiencies for weighted and unweighted events is taken to be the systematic error. In principle, the reweighting procedure could give a larger systematic error if a signal is present in the data. This has been checked by adding signal Monte Carlo, normalized to a cross-section corresponding to the limit of our sensitivity, to the background Monte Carlo and performing the reweighting procedure again. No change in the derived systematic error was observed.

To check the modelling of the variable $\ln y_{23} + 1.4 \cdot \ln y_{12}$, hadronic two-fermion events from the high-energy data have been used. These events have been divided along the plane perpendicular to the thrust axis, and each half reconstructed separately. The distributions for such half-events have been compared between data and simulation, resulting in a 6% systematic error.

The systematic errors for all selection variables are added in quadrature. The total systematic error on the background is 31% for eq final states and 8% for ν q states. The largest contributions are the modelling of the quantity $-q_e \cos \theta_e$

(16%) in the eq case and y_{12} and y_{23} (6%) in the νq case.

The systematic errors on the efficiency are taken into account in the limit using the procedure of Highland and Cousins [27]. The background level is systematically shifted down by the total systematic error ensuring conservative limits.

6 Results

Since no significant excess is observed, limits on the couplings are calculated for both scalar and vector leptoquarks and for those values of the branching ratio to electron-quark final states that are allowed in the case of chiral couplings. The leptoquark cross-section calculated with the program `ERATO-LQ` is taken as input to obtain limits on the couplings. The limit calculations are performed according to the procedure of [28] which takes into account the expected background, the expected mass distribution, the signal efficiencies, and the observed candidates. The upper limits at the 95% CL of the coupling λ as a function of the mass m_{LQ} are given in Figures 4 and 5 for the scalar and vector leptoquark states and for different β_e values. For $\beta_e \equiv 0$ no production in eq collisions is possible. The limits for the states $S_{1/2}(q=-2/3)$ and $V_{1/2}(q=-1/3)$ for $\beta_e \rightarrow 0$ are valid if the assumption of chiral couplings is dropped. If a coupling $\lambda = \sqrt{4\pi\alpha_{em}}$ is assumed, where the electromagnetic coupling constant α_{em} is taken at the mass of the leptoquark, $\alpha_{em}(M_{LQ}) \approx 1/128$, the mass limits range from 183 GeV to 202 GeV depending on the leptoquark state.

In this paper, only the case of chiral couplings is considered. If this constraint is dropped, then the constraints on the branching ratio β_e shown in Table 1 no longer apply. For a given state, the resulting mass limits do not depend strongly on β_e .

7 Conclusions

We have searched for singly-produced leptoquarks in electron-photon interactions at e^+e^- centre-of-mass energies between 189 and 209 GeV using data collected with the OPAL detector at LEP. No evidence is found for the production of these particles. Therefore, limits are set on the coupling λ for scalar and vector leptoquarks as a function of the mass for different branching fractions β_e into eq final states. The λ limits can be directly interpreted also as limits on λ' for squarks in R-parity violating SUSY models with the direct decay of the squark into Standard Model particles.

8 Acknowledgements

We particularly wish to thank the SL Division for the efficient operation of the LEP accelerator at all energies and for their close cooperation with our experimental group. We thank our colleagues from CEA, DAPNIA/SPP, CE-Saclay for their efforts over the years on the time-of-flight and trigger systems which we continue to use. In addition to the support staff at our own institutions we are pleased to acknowledge the
Department of Energy, USA,
National Science Foundation, USA,
Particle Physics and Astronomy Research Council, UK,
Natural Sciences and Engineering Research Council, Canada,
Israel Science Foundation, administered by the Israel Academy of Science and Humanities,
Minerva Gesellschaft,
Benozziyo Center for High Energy Physics,
Japanese Ministry of Education, Science and Culture (the Monbusho) and a grant under the Monbusho International Science Research Program,
Japanese Society for the Promotion of Science (JSPS),
German Israeli Bi-national Science Foundation (GIF),
Bundesministerium für Bildung und Forschung, Germany,
National Research Council of Canada,
Research Corporation, USA,
Hungarian Foundation for Scientific Research, OTKA T-029328, T023793 and OTKA F-023259,
Fund for Scientific Research, Flanders, F.W.O.-Vlaanderen, Belgium.

References

- [1] W. Buchmüller, R. Rückl and D. Wyler, Phys. Lett. B191 (1987) 442.
- [2] J. Kalinowski, R. Rückl, H. Spiesberger and P.M. Zerwas, Z. Phys. C74 (1997) 595.
- [3] M.A. Doncheski and S. Godfrey, Phys. Lett. B393 (1997) 355;
M.A. Doncheski and S. Godfrey, Mod. Phys. Lett. A12 (1997) 1719;
J. Blümlein and E. Boos, Nucl. Phys. Proc. Suppl. B37 (1994) 181.
- [4] OPAL Collab., G. Abbiendi et al, *Search for Single Leptoquark and Squark Production in Electron-Photon Scattering at $\sqrt{s_{ee}} = 189$ GeV at LEP*, CERN-EP-2001-040, accepted by Eur. Phys. J. C.

- [5] Direct searches for single or pair production of leptoquarks:
 OPAL Collab., G. Abbiendi et al, Eur. Phys. J. C13 (2000) 15;
 DELPHI Collab., P.P. Allport et al, Phys. Lett. B446 (1999) 62;
 DELPHI Collab., P. Abreu et al., Phys. Lett. B316 (1993) 620;
 DELPHI Collab., P. Abreu et al., Phys. Lett. B275 (1992) 222;
 ALEPH Collab., D. Decamp et al., Phys. Rep. 216 (1992) 253;
 OPAL Collab., G. Alexander et al., Phys. Lett. B263 (1991) 123;
 L3 Collab, B. Adeva et al., Phys. Lett. B261 (1991) 169.
 Indirect searches for leptoquarks:
 ALEPH Collab., R. Barate et al, Eur. Phys. J. C12 (2000) 183;
 OPAL Collab., G. Abbiendi et al, Eur. Phys. J. C6 (1999) 1;
 L3 Collab, M. Acciari et al, Phys. Lett. B433 (1998) 163.
- [6] H1 Collab., C. Adloff et al., *A search for leptoquark bosons in $e^- p$ collisions at HERA*, DESY-01-094, subm. to Phys. Lett. B;
 ZEUS Collab., J. Breitweg et al., Phys. Rev. D63 (2001) 052002;
 ZEUS Collab., J. Breitweg et al., Eur. Phys. J. C16 (2000) 253;
 H1 Collab., C. Adloff et al., Eur. Phys. J. C11 (1999) 447.
- [7] D0 Collab., V. M. Abazov et al., *Search for leptoquark pairs decaying to $\nu\nu + jets$ in $p\bar{p}$ collisions at $\sqrt{s} = 1.8$ TeV*, FERMILAB-PUB-01-349-E, submitted to Phys. Rev. Lett.;
 D0 Collab., V. M. Abazov et al., Phys. Rev. D64 (2001) 092004;
 D0 Collab., B. Abbott et al., Phys. Rev. Lett. 80 (1998) 2051;
 CDF Collab., F. Abe et al., Phys. Rev. Lett. 79 (1997) 4327;
 D0 Collab., B. Abbott et al., Phys. Rev. Lett. 79 (1997) 4321.
- [8] OPAL Collab., K. Ahmet et al., Nucl. Instr. and Meth. A305 (1991) 275.
- [9] S. Anderson et al., Nucl. Instr. and Meth. A403 (1998) 326.
- [10] OPAL Collab., K. Ackerstaff et al., Eur. Phys. J. C12 (2000) 551.
- [11] B.E. Anderson et al., IEEE Transactions on Nuclear Science 41 (1994) 845.
- [12] OPAL Collab., K. Ackerstaff et al., Phys. Lett. B391 (1997) 221.
- [13] C. Papadopoulos, Comp. Phys. Comm. 118 (1999) 118;
 C. Papadopoulos, Comp. Phys. Comm. 101 (1997) 183.
- [14] T. Sjöstrand, Comp. Phys. Comm. 82 (1994) 74.
- [15] S. Jadach, B.F.L. Ward and Z. Wąs, Comp. Phys. Comm. 79 (1994) 503.
- [16] S. Jadach, W. Płaczek, B.F.L. Ward, in ‘Physics at LEP2’, eds. G. Altarelli, T. Sjöstrand and F. Zwirner, CERN 96-01, Vol. 2 (1996).

- [17] G. Marchesini, B.R. Webber, G. Abbiendi, I.G. Knowles, M.H. Seymour and L. Stanco, *Comp. Phys. Comm.* 67 (1992) 465.
- [18] R. Engel and J. Ranft, *Phys. Rev.* D54 (1996) 4244;
R. Engel, *Z. Phys.* C66 (1995) 203.
- [19] J.A.M. Vermaseren, *Nucl. Phys.* B229 (1983) 347.
- [20] J. Fujimoto et al., in “Physics at LEP2”, eds. G. Altarelli, T. Sjöstrand and F. Zwirner, CERN 96-01, Vol. 2 (1996).
- [21] J. Allison et al., *Nucl. Instr. and Meth.* A317 (1992) 47.
- [22] OPAL Collab., K. Ackerstaff et al., *Z. Phys.* C73 (1997) 433.
- [23] N. Brown and W.J. Stirling, *Phys. Lett.* B252 (1990) 657;
S. Bethke, Z. Kunszt, D. Soper and W.J. Stirling, *Nucl. Phys.* B370 (1992) 310;
S. Catani et al., *Phys. Lett.* B 269 (1991) 432;
N. Brown and W.J. Stirling, *Z. Phys.* C58 (1992) 629.
- [24] OPAL collaboration, R. Akers et al., *Z. Phys.* C63 (1994) 197.
- [25] M. Hauschild et al., *Nucl. Instr. and Meth.* A314 (1992) 74.
- [26] C. Friberg, E. Norrbin, T. Sjöstrand, *Phys. Lett.* B403 (1997) 329 and private communications.
- [27] R.D. Cousins and V.L. Highland, *Nucl. Instr. and Meth.* A320 (1992) 331.
- [28] OPAL Collab., K. Ackerstaff et al., *Eur. Phys. J.* C5 (1998) 19.

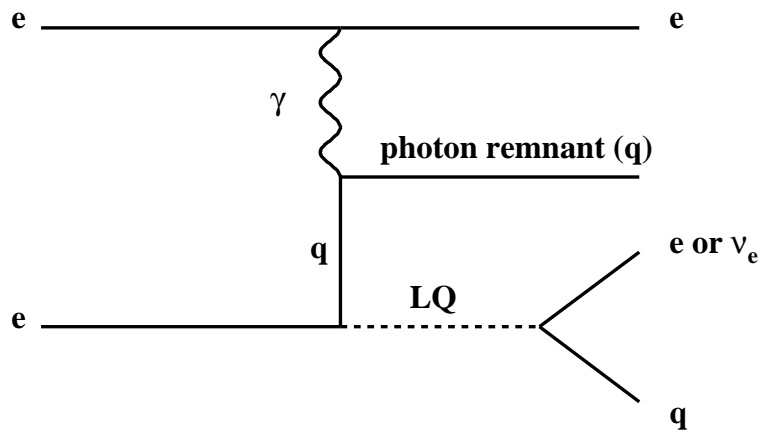


Figure 1: Schematic diagram of the s -channel production of a leptoquark in electron-photon scattering. The photon is radiated by one of the LEP beams, fluctuates into a hadronic object, and one of the quarks interacts with an electron from the other beam.

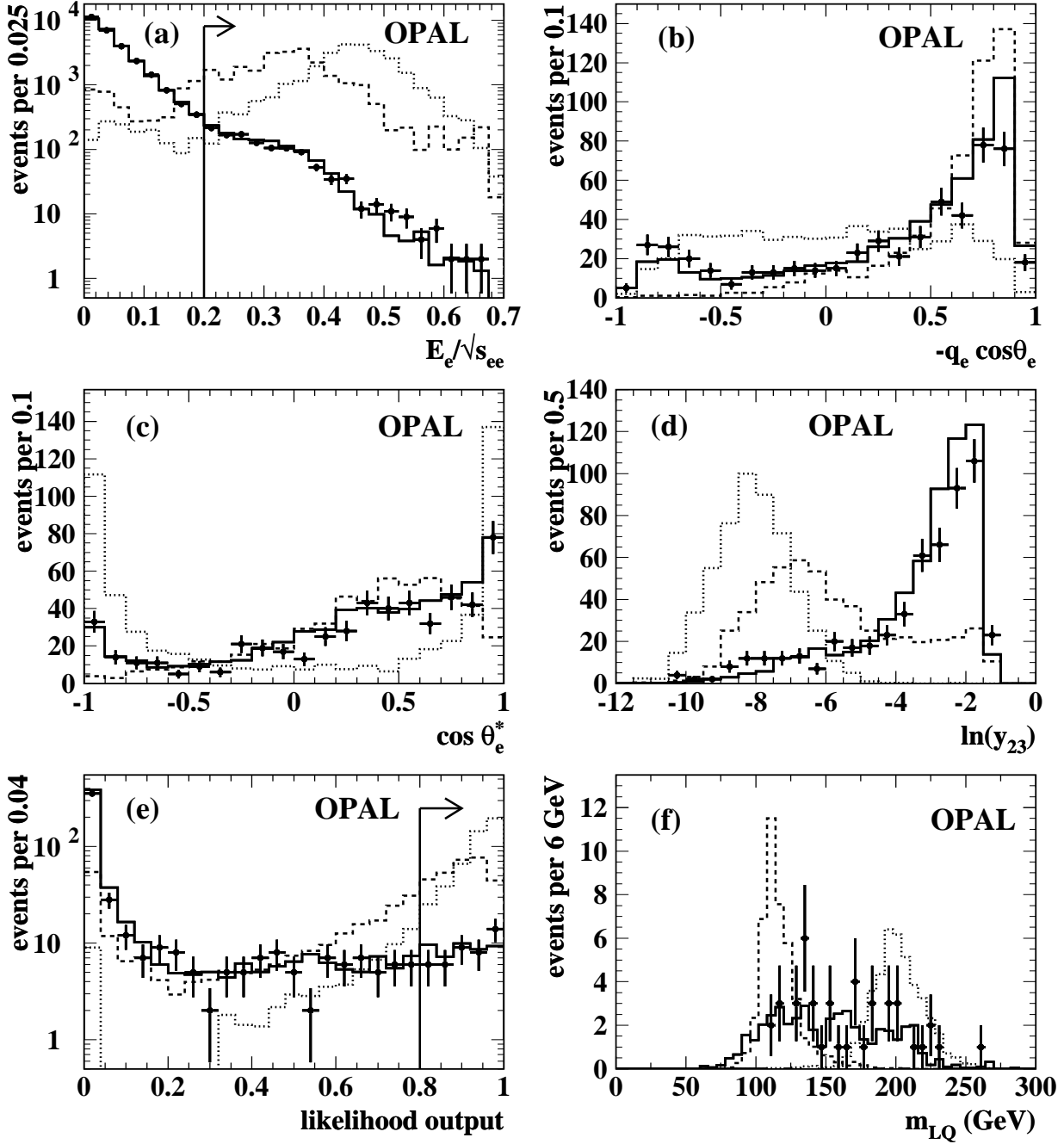


Figure 2: Electron-quark decay channel: (a) distribution of the ratio $E_e/\sqrt{s_{ee}}$ after cut (EQ2); (b)-(d) distributions of the likelihood input variables $-q_e \cos \theta_e$, $\cos \theta_e^*$, and $\ln y_{23}$ after cut (EQ4); (e) distribution of the likelihood output \mathcal{L} after cut (EQ4); (f) mass distribution of the selected leptoquark candidates after the full selection. The points with error bars are the data and the full line represents the total Standard Model background normalised to the data luminosity. The dashed and dotted histograms show the distribution for the scalar state $S_{1/2}$ at $\sqrt{s_{ee}} = 200$ GeV with scaled masses of $x_{LQ} = 0.53$ and $x_{LQ} = 0.95$, respectively. The normalisation of the leptoquark signals is arbitrary. In plots (a) and (e), the arrow points into the accepted region.

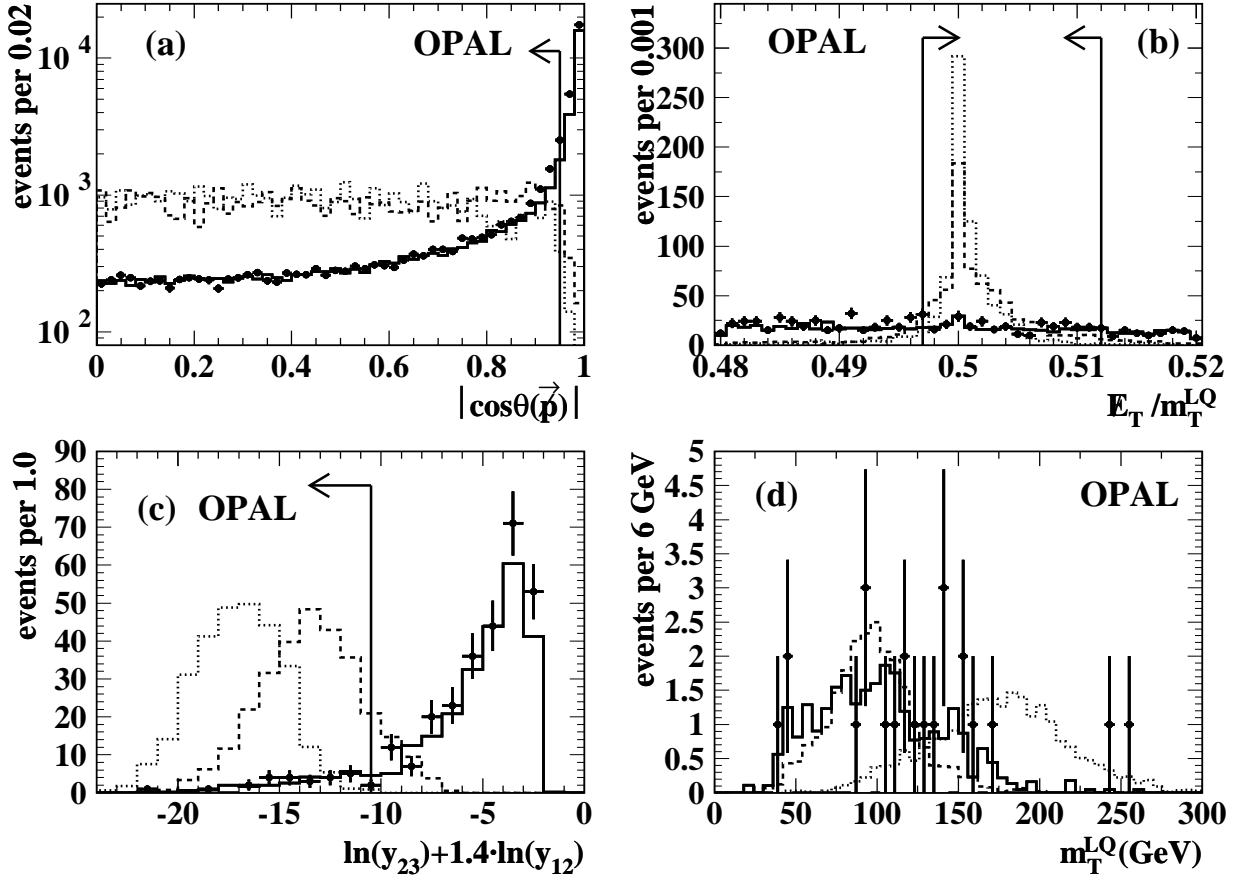


Figure 3: Neutrino-quark decay channel: (a) $|\cos\theta(\vec{p})|$ distribution after cut (NQ1); (b) distribution of the variable E_T/m_T^{LQ} after cut (NQ2); (c) distribution of the variable $\ln y_{23} + 1.4 \ln y_{12}$ after cut (NQ3); (d) transverse mass distribution of the selected leptoquark candidates after the full selection. The points with error bars are the data and the full line represents the total Standard Model background normalised to the data luminosity. The dashed and dotted histograms show the distribution for the scalar state $S_{1/2}$ at $\sqrt{s_{ee}} = 200$ GeV with scaled masses of $x_{LQ} = 0.53$ and $x_{LQ} = 0.95$, respectively. The normalisation of the leptoquark signals is arbitrary. In plots (a), (b), and (c), the arrow points into the accepted region.

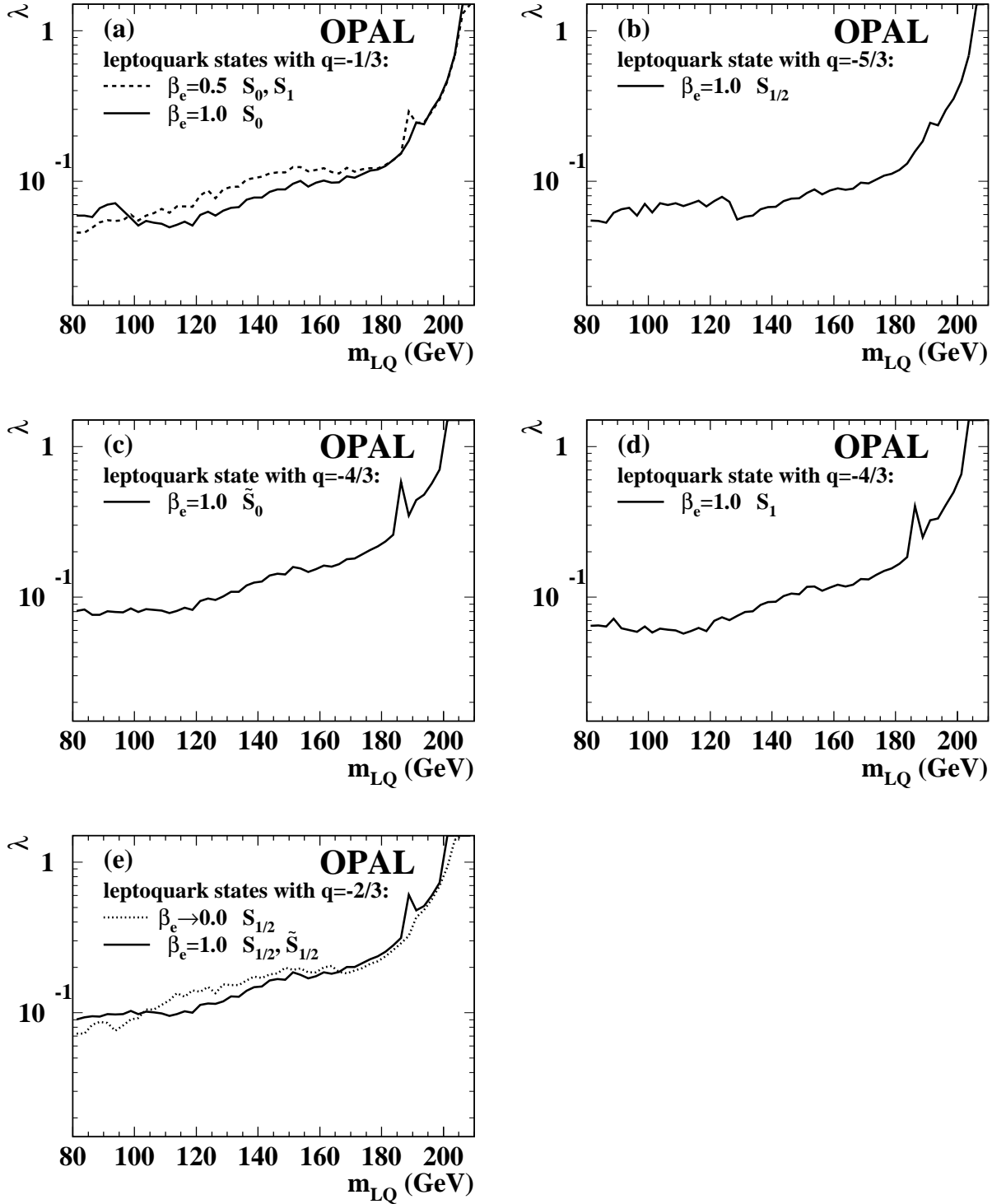


Figure 4: Upper limits at 95% confidence level on the coupling constant λ for single production of the scalar leptoquark states for different branching fractions β_e .

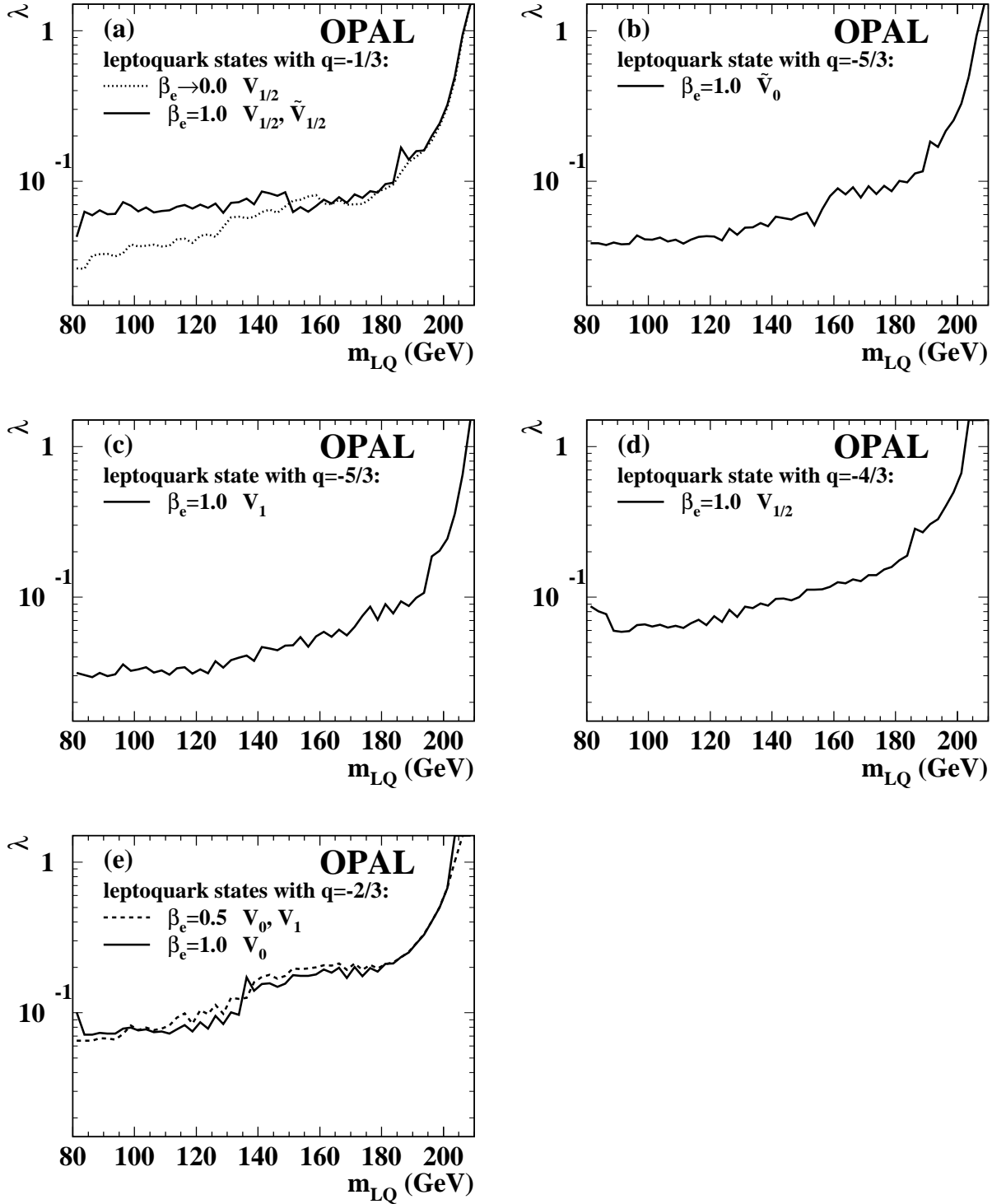


Figure 5: Upper limits at 95% confidence level on the coupling constant λ for single production of the vector leptoquark states for different branching fractions β_e .